Interaction of oxygen with silver at high temperature and atmospheric pressure: A spectroscopic and structural analysis of a strongly bound surface species

X. Bao, M. Muhler, Th. Schedel-Niedrig,* and R. Schlögl
Fritz-Haber-Institut der Max-Planck-Gesellschaft, Faradayweg 4-6, D-14195 Berlin (Dahlem), Germany
(Received 16 February 1996)

X-ray photoelectron spectroscopy, ultraviolet photoelectron spectroscopy (UPS), and ion scattering spectroscopy (ISS) have been used to study the Ag(111) single-crystal surface after exposure to O_2 at high temperature and at atmospheric pressure. The activated formation of a strongly bound surface layer has been observed, as identified by an asymmetry of the Ag $3d_{5/2}$ core-level peak at 367.3 eV and an O 1*s* peak at 529.0 eV (O_γ). In addition, oxygen was found to be dissolved in the bulk (O_β), exhibiting an O 1*s* binding energy between 531 and 530 eV depending on its abundance. X-ray-excited oxygen *KVV* Auger electron spectroscopy revealed the presence of O_γ by additional peaks at 514.8 and 494.7 eV. UPS displayed oxygen-derived bands located above the emission from the Ag 4*d* band at 3.2 and 2.5 eV. Oxygen-related peaks below the Ag 4*d* band were identified as resulting from OH groups formed by reaction of surface oxygen (O_α) with residual hydrogen. The incorporated oxygen caused a pronounced charge separation as reflected by a 1 eV increase in the work function. ISS measurements revealed that O_γ is incorporated in the topmost surface layer, shielding underlying Ag atoms from the He^+ beam. All spectroscopic data point to the presence of one monolayer of silver-embedded oxygen, which is in dynamic equilibrium with surface atomic oxygen segregated from the bulk at high temperature. The oxygen embedded in the topmost silver layer is strongly bound to the metal, with its interaction being different from adsorbed atomic oxygen and bulk Ag_2O. It is stable up to 900 K, in contrast to the binary silver oxides, and relevant for high-temperature oxidation reactions catalyzed by Ag. A qualitative analysis is presented of the chemical bonding of the different surface species in comparison to the situation of a complex silver oxide reference. [S0163-1829(96)09527-6]

I. INTRODUCTION

The interaction of oxygen with silver has already been the subject of numerous studies because of its unique catalytic relevance for several large-scale industrial processes. Silver is mainly used for the epoxidation of ethylene[1] and for the partial oxidation of methanol to formaldehyde.[2] On Ag(110) the following reaction scheme is generally accepted.[3] At a temperature of 25 K O_2 adsorbs into the physisorbed precursor state with some formation of the molecular chemisorbed state. On warming, the physisorbed state desorbs and/or partly converts. At 170 K, the chemisorbed state also partly desorbs and partly dissociates into the atomic state (labeled O_α) which recombines and desorbs, leaving an uncovered surface at temperatures above 580 K. Increasing the oxygen dosing temperature may lead to the absorption of oxygen into the bulk (labeled O_β). Heating bulk-loaded silver causes segregation of O_β and conversion to O_α with subsequent partial desorption. Heating oxygen-covered surfaces of silver clean in the bulk causes dissolution of oxygen atoms into the bulk in addition to desorption. Bulk atomic oxygen species can thus be interconverted and, e.g., interfere with each other in thermally stimulated desorption (TDS) experiments.[4]

Studies of the interaction on Ag(111) with oxygen are rendered difficult by the much lower sticking coefficient of about 10^{-6} for O_α, requiring high-pressure dosing.[5] Recently, *in situ* oxidation of Ag yielding Ag_2O was achieved by exposing Ag(110) to a dc glow discharge plasma[6] or by exposing Ag(111) to a free-radical oxygen source (cold discharge, magnetically confined).[7]

In the course of an ongoing study of the silver-oxygen system for the partial oxidation of methanol, it has been found that oxygen exposure at or near atmospheric pressure and at temperatures $\geqslant$800 K leads to a pronounced restructuring of the Ag(111) surface, with a superlattice given in matrix notation as $(26\times1;-1\times26)$, which was characterized by reflection electron microscopy (REM), reflection high-energy electron diffraction (RHEED), and scanning tunneling microscopy (STM).[8–10] Associated with the distorted silver lattice, a tightly held oxygen species with a desorption temperature above 900 K and a Ag-O vibrational frequency at $\sim$800 cm^{-1} was formed. This strongly bound oxygen species (labeled as O_γ) was identified under conditions close to those used in the catalytic oxidation of methanol to formaldehyde by *in situ* Raman spectroscopy, and was therefore suggested to be the active site responsible for the methanol dehydrogenation.[9] In the present investigation, the Ag(111) surface has been characterized by the combined application of x-ray photoelectron spectroscopy (XPS), ultraviolet photoelectron spectroscopy (UPS), and ion scattering spectroscopy (ISS) after exposure to O_2 at atmospheric pressure and at high temperature. Under these conditions, the formation of the catalytically relevant O_γ species can be expected. The spectroscopic data will be used to locate and characterize the bonding interaction of this form of oxygen on silver, which is not accessible under standard ultrahigh-vacuum (UHV) gas exposure conditions. The Ag(111) surface was chosen for the present study as earlier experiments showed that O_γ requires for its formation a hcp silver surface. Providing this as a single crystal should reduce the abundance of surface

atomic oxygen O_α, and hence facilitate spectral interpretation.

II. EXPERIMENTAL DETAILS

Experiments were carried out on a Ag(111) single crystal surface prepared by standard polishing procedures. Prior to oxygen exposure, it was treated by cycles of Ar^+ ion sputtering (1 kV, 2 μA) and subsequent annealing up to 780 K. This process was repeated until sharp low-energy electron diffraction (LEED) spots, indicating a well-ordered (111) lattice, were obtained and no other contamination except traces of oxygen (less than 2%) could be detected by Auger electron spectroscopy (AES). The spectroscopic investigations were performed with a modified Leybold LHS 12 MCD system equipped with facilities for UPS, XPS, ISS, and TDS.[11] Oxygen with a purity of 99.9996% was supplied by Linde. A stainless steel UHV gas inlet system was used. The Ag(111) crystal was clamped to a stainless steel transfer rod by means of tantalum foil. Exposure to oxygen at atmospheric pressure was performed in a preparation chamber with a base pressure of 1×10^{-9} mbar. Prior to pumping down to UHV, the sample was rapidly cooled to 500 K. Then the sample was transferred within 1 min into the UHV analysis chamber. The XPS data were acquired with Mg $K\alpha$ radiation ($h\nu$ $=1253.6$ eV) using a fixed analyzer pass energy of 108 eV corresponding to a full width at half maximum (FWHM) of the Ag $3d_{5/2}$ peak of 1.0 eV. Binding energies were calibrated using Au $4f_{7/2}=84.0$ eV. Surface compositions were calculated after subtraction of a Shirley-type background using the cross sections from Ref. 12. He I ($h\nu=21.2$ eV) and He II ($h\nu=40.8$ eV) spectra were acquired using analyzer pass energies of 12 and 24 eV, respectively. The work function of the sample was obtained by measuring the cutoff of the He I spectrum.[13] In order to minimize the sputtering damage, the ISS data were generated using a scanning defocused 100 eV He^+ primary beam and a minimized acquisition time of 60 s. The impinging He^+ current under these quasistatic conditions was about 1 μA, corresponding to an ion dose of 6×10^{12} ions/cm^2 s.

III. RESULTS

A. Core-level photoemission and Auger electron spectroscopy

It was found[8] by STM and REM that exposure of Ag(111) to O_2 at atmospheric pressure and at high temperature caused pronounced restructuring of the surface region associated with the formation of a strongly held oxygen species desorbing only above 900 K. Figure 1 presents the O 1s XPS data from a Ag(111) surface after prolonged exposure to 1 bar oxygen at different temperatures. All O 1s spectra shown are normalized to the same Ag 3d intensity. The exposure at 450 K for 5 h gave rise to a single O 1s peak centered at 530.4 eV exhibiting a FWHM of about 1.5 eV (Fig. 1, curve a). It is known that long oxygen exposures at high pressure may lead to an adlayer dominated by carbonate and hydroxyl groups.[14] The presence of carbonate species can safely be excluded, based on the absence of the corresponding C 1s peak at 287.7 eV,[14,15] and the exposure temperature of 450 K at which the preparation chamber was evacuated after the treatment. Strongly bound H_2O/OH species may indeed contribute to the O 1s peak, giving rise to the tailing to higher binding energy as discussed later in connection with the UPS data. The binding energy of adsorbed atomic oxygen (O_α) is controversial in the literature. The determined values range from about 528 to 530.3 eV (see references in Ref. 11), which may be related to the embedding of O_α in the surface as suggested by, e.g., Joyner and Roberts,[16] Grant and Lambert,[17] and Rehren *et al.*,[11] who also pointed out the influence of dissolved oxygen. The assignment of the observed O 1s peak to O_α is supported by its desorption temperature of about 620 K.[11] After the exposure at 580 K for 5 h (Fig. 1, curve b) the shape of the O 1s peak was found to be changed, indicating the development of a new component labeled as O_γ in Fig. 1 at a binding energy of about 529.1 eV close to the value of 528.9 eV reported for Ag_2O.[7] Raising the exposure temperature to 680 K (Fig. 1, curve c) and further to 780 K (Fig. 1, curve d and e) and caused the O_γ peak to rise. The 530.4 eV peak representing chemisorbed atomic oxygen diminished with increase of exposure time, and a pronounced tailing to higher binding energy emerged instead. After an exposure time of 7 h at 780 K (Fig. 1, curve f), a second peak (labeled O_β) became more clearly visible at about 530.5 eV. In Fig. 1, curve g, an O 1s spectrum obtained after dosing at 780 K is shown, which was measured at 780 K demonstrating the high thermal stability of O_γ.

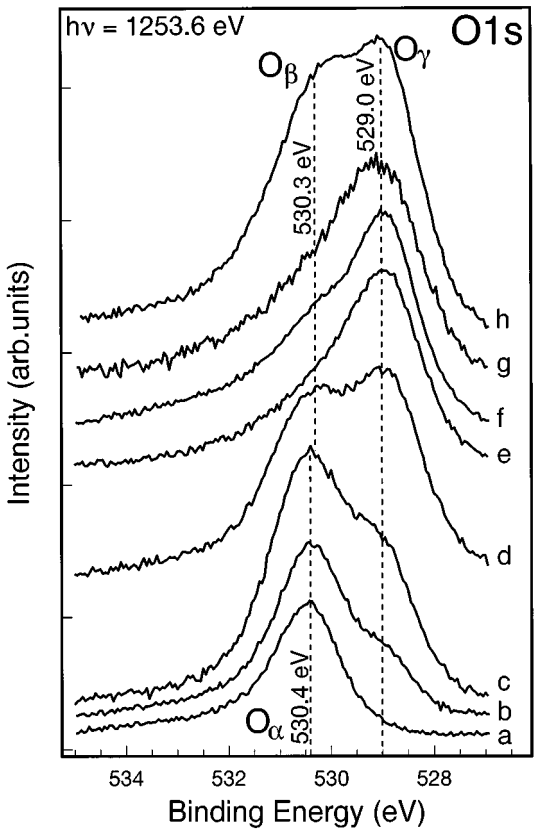

FIG. 1. O 1s core-level data from a Ag(111) surface after exposure to 1 bar O_2 for 5 h: curve a at 450 K; curve b at 580 K; curve c at 680 K; curve d at 780 K for 3 h; curve e at 780 K for 5 h; curve f at 780 K for 7 h; curve g after preparation, curve f detected at 780 K; and curve h after exposure to 1 bar O_2 for 5 h at 900 K.

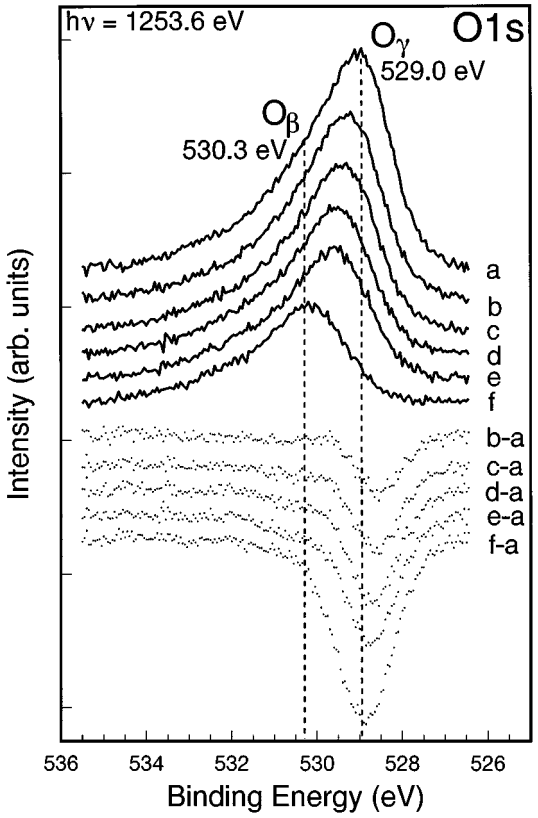

FIG. 2. A sequence of O 1*s* core-level data from a Ag(111) surface. Curve *a*, initially exposed to 1 bar O_2 for 7 h at 780 K and, curves *b*–*f*, after *consecutive* 5 min exposure to soft He^+ sputtering with 1 keV primary energy (10 μA). The difference spectra shown at the bottom of the figure were obtained by subtracting the spectrum of the indicated sputtered surface from the initial spectrum *a*.

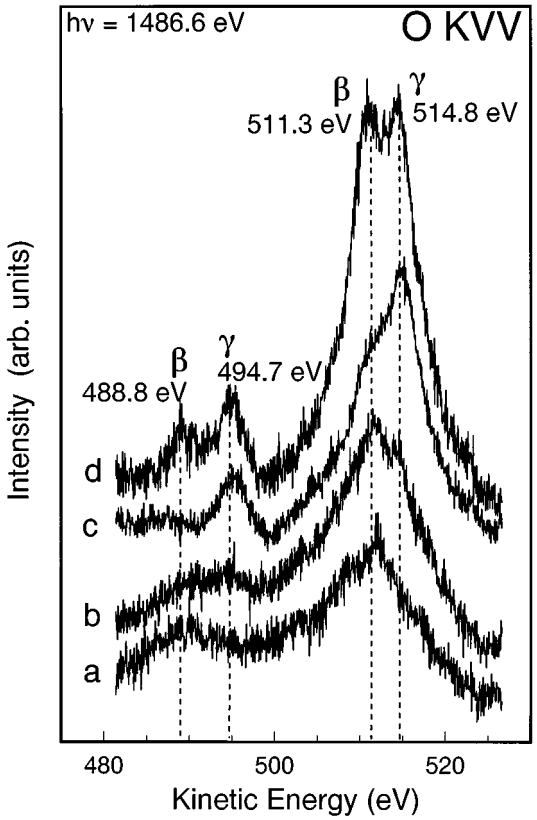

FIG. 3. O *KLL* Auger electron data from a Ag(111) surface after exposure to 1 bar O_2 for 5 h: curve *a* at 450 K; curve *b* at 580 K; curve *c* at 750 K; and curve *d* at 900 K.

When raising the exposure temperature to 900 K (Fig. 1, curve *h*) the O_γ O 1*s* peak was found to be more or less unchanged in its intensity and position. However, the O_β peak grew markedly and shifted towards lower binding energies. The total O/Ag ratio increased from 0.2 after dosing at 450 K to 0.3 after dosing at 780 K, finally reaching 0.5 after the treatment at 900 K, which corresponds formally to the stoichiometry of Ag_2O.

In Fig. 2 the result of a depth profiling experiment is displayed, which enables us to determine the relative location of the O_γ and O_β species. A scanning He^+ ion gun was used with 1 keV primary energy for gentle sputtering. A sequence of O 1*s* spectra was measured after the initial O_2 exposure at 780 K (Fig. 2, curve *a*) followed by exposure to the He^+ ion beam for the periods of time specified (Fig. 2, curves *b*–*f*). The difference spectra Fig. 2, curve *b*−*a* and Fig. 2 curve *c*−*a* reveal clearly that the O_γ species is sputtered off first. After prolonged sputtering the O 1*s* peak related to O_β at 530.3 eV binding energy also started to decrease (Fig. 2, curve *f*−*a*). Hence the depth profiling experiment supports the localization of O_γ in the surface layer and O_β being dissolved in the bulk. The O_γ species is identified by a symmetric peak at 529.0 eV with a FWHM of about 1.6 eV as shown in Fig. 2, curves *f*−*a*. Attempts to fit the remaining asymmetric O_β peak with a single Gauss-Lorenzian peak resulted in a FWHM of about 3.5 eV. Based on the charge-potential model[18] it is obvious that the binding energy of a dissolved species should depend on its concentration, resulting in a distribution of binding energies in the case of a concentration gradient into the bulk.

Attempts were made to localize O_β and O_γ by varying the exit angle of electron emission relative to the hemispherical analyzer. Although the XPS results seemed to indicate overlayer characteristics for O_γ, the interpretation of the results remained inconclusive. This is ascribed to the roughening of the Ag surface on the micrometer scale due to the high-temperature and high-pressure O_2 exposure.[19]

A series of O *KVV* Auger spectra (Fig. 3) excited by Al $K\alpha$ x-ray radiation ($h\nu$=1486.6 eV) was recorded after varied O_2 exposures, to investigate the correlation between lineshape changes of the O 1*s* peak and the Auger O *KVV* transition involving the O 1*s* core level and the valence band. Figure 3, curve *a*, shows the spectrum after the exposure to 1 bar O_2 for 5 h at 450 K. Two additional peaks at 514.8 and 494.7 eV associated with O_γ emerged after O_2 dosing at 580 K, as shown in Fig. 3, curve *b*. The higher kinetic energy of the O_γ-related O *KVV* peaks provides some evidence for an oxidelike nature of O_γ, since for Ag_2O the kinetic energy of O $KL_{23}L_{23}$ was found to be 513.9 eV. The features related to O_γ at 514.8 and 494.7 eV increased after raising the temperature to 750 K (Fig. 3, curve *c*). The two peaks associated with the O_β peak at 511.3 and 488.8 eV were found to increase when dosing at 900 K. The slight difference in the intensity ratio of O_β and O_γ between XPS and AES measurements is attributed to the different mean free paths of the emitted electrons. The O *KVV* Auger electrons have a lower

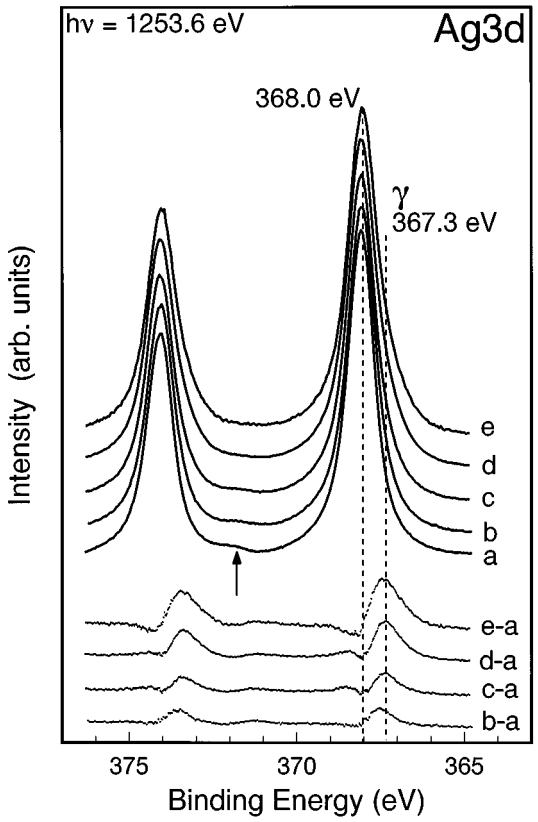

FIG. 4. Ag $3d$ core-level data. Curve a from a clean Ag(111) surface, and after exposure to 1 bar O_2 for 5 h at (curve b) 450 K, (curve c) 580 K, (curve d) 750 K, and (curve e) 900 K. The difference spectra were obtained by subtracting the intensity of the clean surface from that of the corresponding oxygenated surfaces.

kinetic energy than the O $1s$ electrons, leading to a higher surface sensitivity of the AES measurements.

The formation of a surface layer of strongly interacting oxygen as evidenced by the growth of the O_γ species with the increasing temperature and duration of the oxygen exposure is expected to affect the Ag $3d$ peak shape also. The strong electron affinity of oxygen should lead to an electron transfer to the adsorbed oxygen atoms, giving rise to positively charged metal atoms. Upon oxidation, the observed core-level binding energies for most transition metals are shifted towards higher binding energies.[20] Silver, however, is one of the few examples for a lowered binding energy in the oxidized state.[7] Figure 4 presents a series of Ag $3d$ core-level spectra obtained after oxygen treatments at various temperatures as indicated in the figure. The positions of the peak maxima remained unchanged at 368.0 eV. The arrow in Fig. 4 points to a satellite structure at 3.65 eV higher binding energy, which is due to plasmon excitation. Upon oxidation, its intensity decreases and after oxygen exposure at 900 K (Fig. 4, curve e) it is virtually absent, as is the case for Ag_2O.[7] The shape of the Ag $3d$ peaks was found to be changed, exhibiting a growing asymmetry to lower binding energy with increasing oxygen exposure temperature. Such oxygen-induced changes of the Ag $3d$ peak shape can be seen more clearly in the corresponding difference spectra obtained by subtracting the normalized spectrum of clean Ag(111) (Fig. 4, curve a) from the oxygen-exposed spectra. An additional Ag $3d_{5/2}$ peak emerges at about 367.3 eV, the intensity of which is roughly correlated with the growth in intensity of the O $1s$ peak. After the treatment at 450 K the feature reveals only small intensity and can be attributed to the presence of adsorbed and dissolved atomic oxygen species; after the high-temperature treatment the peak exhibits a strongly pronounced intensity. Corresponding shifts of the Ag $3d$ peaks by 0.5–0.8 eV to lower binding energy were observed after exposing Ag single crystals to an oxygen plasma.[6,7] Again, the similarity between the Ag $3d$ spectra obtained after dosing oxygen at atmospheric pressure and Ag $3d$ spectra from well-defined Ag_2O allows us to suppose the existence of a layer of oxygen-saturated Ag(111), although the exposure temperature was higher than the bulk decomposition temperature of Ag_2O of about 600 K.[6,7] This indicates that we have obtained an oxygen species with a different chemical bonding than in binary oxides. As shown in Fig. 4, the Ag $3d$ difference spectrum $(e-a)$ accounts for about 13% of the total integrated area of spectrum e. This intensity ratio enables us to estimate the thickness of the O_γ layer. The monolayer thickness of Ag is given by

$$a^3 = M_{\mathrm{Ag}}/(\rho_{\mathrm{Ag}} N_A) \tag{1}$$

where M_{Ag} is the Ag molar weight of 107.9 g/mol, ρ_{Ag} is the Ag density of 10.5 g/cm^3, and N_A is the Avogadro number, yielding $a=2.6$ Å. For elements, the following equation for the inelastic mean free path (IMFP) λ was determined:[21]

$$\lambda = 538E_k^{-2} + 0.41(aE_K)^{0.5} \ \text{(monolayers)}, \tag{2}$$

where E_K is the kinetic energy of the emitted photoelectron. For a Ag $3d_{5/2}$ photoelectron, E_K is equal to 885.6 eV, yielding an IMFP of about six monolayers. Hence the first monolayer contributes 15% to the total intensity, suggesting that the O_γ surface layer has a thickness of one monolayer.

B. Valence-band photoemission

The results obtained by UPS are summarized in Figs. 5 and 6 using He I and He II radiation, respectively. After the exposure of the clean Ag(111) surface (Fig. 5, curve a) to oxygen at 780 K for 1 h (Fig. 5, curve b), the valence-band spectrum was drastically modified, resulting in a strong perturbation of the Ag $4d$ main doublet. Additional features appeared above the Ag $4d$ band at 3.2 eV and also below the Ag $4d$ band at 9.8 eV. The corresponding He II spectrum shown in Fig. 6, curve b, clearly reveals an additional peak to the 9.8 eV feature at 12.5 eV below Ag $4d$. Using the known energy dependence of the photoionization cross section, it is possible to estimate the O $2p$ character of the observed bands. The atomic cross sections weighted by the number of electrons per atom are $\sigma(\mathrm{O}\ 2p/\mathrm{Ag}\ 4d)=1.0$ and 0.3 for He I and He II radiation, respectively.[12] From the He I and He II spectra, the relative decrease in intensity of the oxygen-induced peaks compared to the Ag $4d$ band indicates that the O $2p$ character of the features below the Ag $4d$ band is considerably higher than that of the features above the Ag $4d$ band. Based on this observation and the absence of any additional structures below the Ag $4d$ band observed for Ag_2O (Ref. 7) and oxygen-covered Ag(110) (Ref. 22) we assign the peaks at 9.8 and 12.5 eV to OH/H_2O species. In

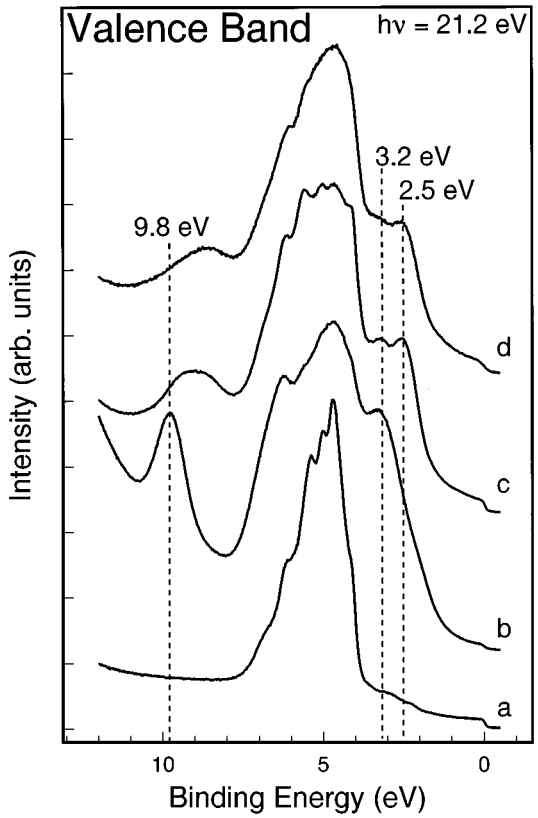

FIG. 5. Valence-band data excited with He I ($h\nu$=21.2 eV) radiation from (curve *a*) a clean Ag(111) surface, and after exposure to 1 bar O_2 (curve *b*) at 780 K for 1 h and (curve *c*) at 780 K for 12 h. The spectrum *d* was detected at 780 K after the preparation *c*.

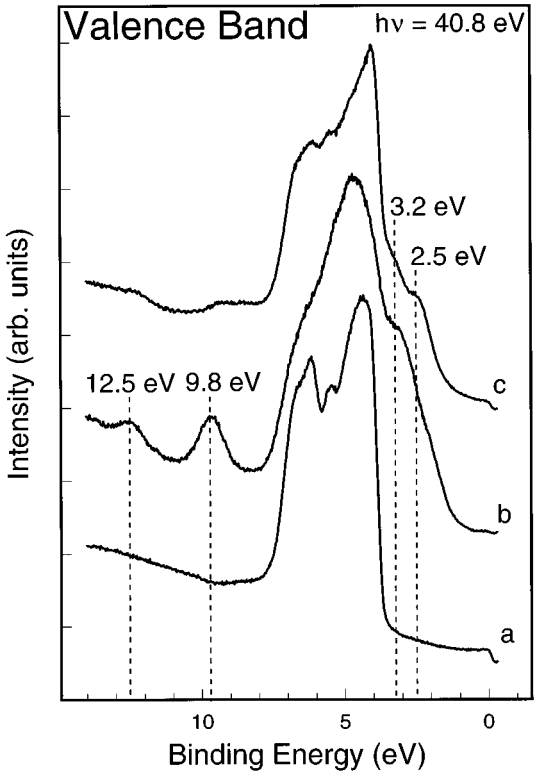

FIG. 6. Valence-band data excited with He II ($h\nu$=40.8 eV) radiation from (curve *a*) a clean Ag(111) surface, and after exposure to 1 bar O_2 (curve *b*) at 780 K for 1 h and (curve *c*) at 780 K for 12 h.

earlier experiments with an oxygen-exposed silver foil treated suitably with oxygen and hydrogen[11] a high reactivity of this O_α species towards hydrogen and the formation of surface OH was observed. In a recent temperature programmed reaction spectroscopy (TPRS) study of a polycrystalline silver catalyst with hydrogen, the selective reactivity of the O_α species with hydrogen to OH/H_2O and the complete inactivity of O_γ were reported.[4,23] The coverage of the present Ag(111) surface with active oxygen being formed by direct chemisorption or resulting form segregation of O_β to parts of the surface not covered with O_γ can be estimated from the abundance of the OH species. The distance between the two peaks of 2.7 eV and their intensity ratio of about 2.3 further suggest their assignment as OH groups.

Upon prolonging the oxygen exposure to 13 h at 780 K (Fig. 5 curve, *c*) a second peak at 2.5 eV appeared more clearly, whereas the peak at 9.8 eV lost intensity and shifted to 9.1 eV. Comparing the shape of the Ag 4*d* band in spectrum *c* of Fig. 5 with spectrum *a* of Fig. 5 indicates that the Ag(111) single-crystal surface is transformed to a polycrystalline surface due to oxygen-induced faceting.[19] The increased surface abundance of facets with O_γ is reflected by the reduced coverage with OH caused by O_α, which indicates that on surface patches transformed into Ag-O_γ there is no additional surface atomic oxygen O_α present.

The shape and intensity ratio of the two structures at 3.2 and 2.5 eV curve *c* in Figs. 5 and 6 closely resemble those observed for Ag_2O at 2.8 and 1.8 eV,[7] supporting the suggested oxidelike nature of O_γ. The unexpected thermal stability of the O_γ layer is demonstrated by spectrum *d* in Fig. 5, which was measured at 780 K. The layer thickness of about one monolayer is supported by the presence of the Fermi edge in spectra *b* and *c* in Figs. 5 and 6. The IMFP of electrons excited with He II radiation and emitted from the Fermi edge can be estimated to be only two monolayers.[21] Obviously, the overlayer is not thick enough to shield the emission from metallic Ag underneath. A pronounced increase of the work function due to the presence of the O_γ layer was observed by recording the onset of the secondary electron emission in the He I excited valence-band spectra.[13] After oxygen dosing at 450 K the increase of the work function was found to be about +0.55 eV, which is in fair agreement with the values reported for the saturated adsorption of atomic oxygen on silver surfaces.[2] The work function increased from 0.6 to about 1 eV when the oxygen exposure was carried out at 780 K causing formation of the O_γ species on the surface. Segeth, Wijngaard, and Sawatzky[24] observed an increase of 1.3 eV in the presence of ''strongly bound oxygen'' obtained after oxygen dosing at 100 mbar for 30 min above 470 K. Furthermore, these authors demonstrated by an isochronal annealing sequence that the work function change is correlated with the valence-band peak at 3.1 eV.[24] The correlation between the work function change and the presence of O_γ was further confirmed in the present study by dosing with methanol at 780 K.[9] The removal of O_γ by reaction with methanol was found to restore the work function of metallic Ag although O_β was still present.

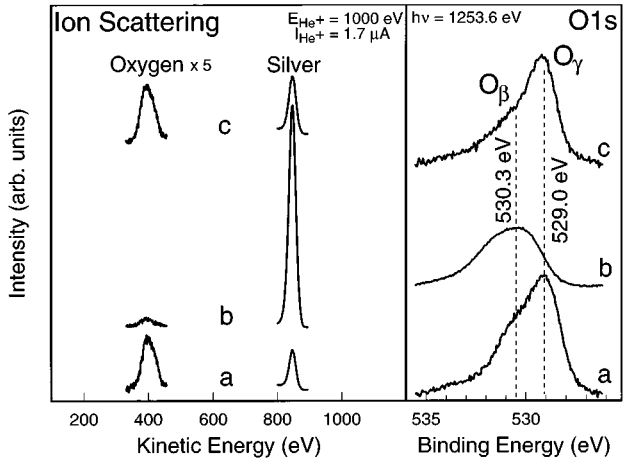

FIG. 7. Ion scattering spectroscopy and O 1*s* core-level data from a Ag(111) surface after different treatments: (curve *a*) after exposure to 1 bar O_2 at 750 K for several hours; (curve *b*) after sputtering of the initial state *a* by He^+ ions (1000 eV, 10 μA) for 5 min at 300 K; (curve *c*) after heating of the state *b* at 750 K for 30 min in UHV.

C. Ion scattering spectroscopy

Further evidence for the location of O_γ embedded in the topmost silver layer was provided by applying ion scattering spectroscopy. This technique is known to be exclusively surface sensitive since only the topmost atoms can contribute to the scattered He^+ ion intensity. During the measurement, however, the surface is consecutively sputtered off, thus exposing deeper layers to the incident beam with ongoing time. Hence depth profiling is possible by acquiring sequences of IS spectra with a short accumulation time for each spectrum. Based upon the description by Niehus, Heiland, and Taglauer,[25] the scattering intensity from a clean Ag surface (I^0_{Ag}) can been expressed, when neglecting the shadow- or blocking-cone trajectory focusing, as

$$I^0_{\mathrm{Ag}}=(d\sigma/d\Omega)I_0P^+T\Delta\Omega N^0_{\mathrm{Ag}} \tag{3}$$

where I_0 is the primary ion current, $d\sigma/d\Omega$ the cross section for scattering into a solid angle $\Delta\Omega$, T the transmission factor characterizing the spectrometer, and P^+ the ion survival probability. Given the oxygen surface density N_{oxy} with a shadowing factor α on the Ag surface, the scattering intensity from the uncovered Ag surface ($I^{\mathrm{uncov}}_{\mathrm{Ag}}$), by neglecting the adsorbate-induced change in P^+, will be

$$I^{\mathrm{uncov}}_{\mathrm{Ag}}=(d\sigma/d\Omega)I_0P^+T\Delta\Omega(N^0_{\mathrm{Ag}}-\alpha N_{\mathrm{oxy}}). \tag{4}$$

The slopes obtained from the correlation of the ISS peak areas with each other demonstrated by plotting the Ag peak areas versus the corresponding O peak areas are thus determined by the largely differing ion survival probabilities on oxygen and silver and the shadowing factor α, which is known to range from 1 to 4.[25]

Figure 7 presents a summary of ISS data obtained after different treatments of Ag(111). In comparison with the ISS data, the corresponding O 1*s* core-level spectra are shown in the right part of Fig. 7. The IS spectrum *a* displayed in Fig. 7 originates from an oxygen-saturated Ag(111) surface prepared by exposure to 1 bar O_2 at 780 K for 5 h. It consists of

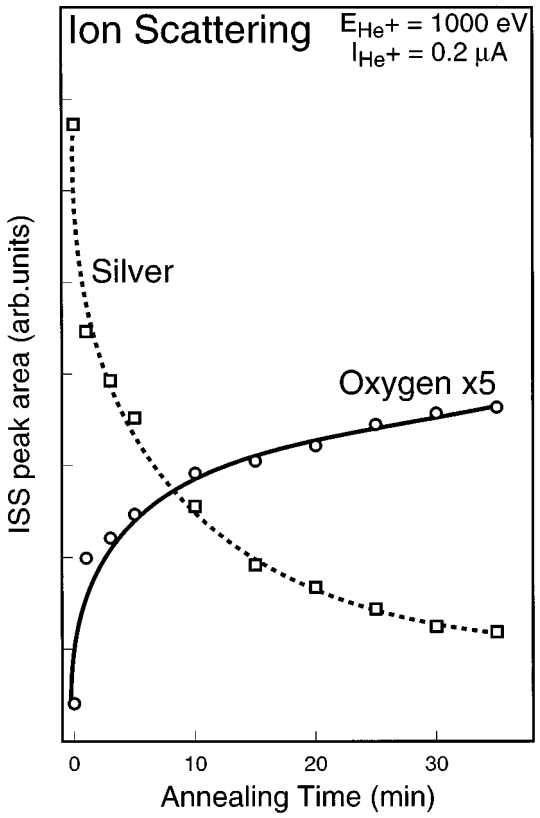

FIG. 8. The variation of the silver and oxygen scattering intensities under quasistatic measurement conditions as a function of the annealing time at 780 K.

two peaks due to scattering from oxygen at $E/E_0=0.4$ and from silver at $E/E_0=0.846$. After gentle sputtering with He^+ ions (1000 eV, 10 μA) for 10 min at room temperature, the oxygen peak has disappeared almost completely (see curve 7*b*). The corresponding O 1*s* core-level spectrum also reveals that the O_γ peak has disappeared. The O 1*s* core-level peak attributed to bulk oxygen O_β, however, was essentially unaffected by the sputtering. This demonstrates that the oxygen ISS peak results essentially from scattering from the O_γ species. The following ISS experiment was performed to monitor the formation of O_γ by diffusion of O_β from the bulk to the surface at 780 K. After the removal of O_γ by sputtering at room temperature (Fig. 7, curve *b*) the ''clean'' surface was heated to 780 K within 20 s and kept at this temperature for 1 h. After the annealing at 780 K (Fig. 7, curve *c*) the IS spectrum displays a pronounced oxygen peak and a strongly decreased silver peak. Associated with the reappearance of the oxygen ISS peak, the O 1*s* core-level peak at 529.0 eV was again observed by XPS, corresponding to curve *a* of Fig. 7. This experiment demonstrates that the O_γ layer was restored during annealing.

The kinetics of this process were studied in more detail by monitoring the variation of the scattering intensities under quasistatic measurement conditions as a function of the annealing time at 780 K. As shown in Fig. 8, the oxygen peak area increased rapidly during the first few minutes, followed by a slower growth approaching the maximum intensity after about 40 min. Correspondingly, the Ag peak area was found to decrease rapidly in the beginning of the annealing experi-

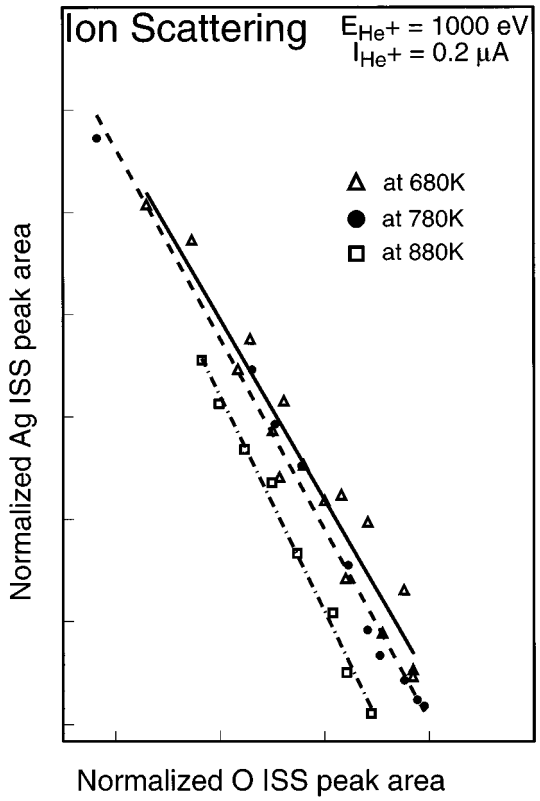

FIG. 9. Correlation of the ion scattering intensities between surface silver and surface oxygen. The linear function, reflected by direct shadowing of the oxygen atoms to the silver substrate, confirms the adsorption of O_γ on the topmost layer of silver.

ment, followed by a slower decrease until steady state was reached after about 40 min. In Fig. 9 the correlation of the ISS peak areas with each other is demonstrated by plotting the Ag peak areas versus the corresponding O peak areas obtained at 680, 780, and 880 K after normalizing to the same He^+ ion dose. A linear correlation is obtained for all three temperatures, i.e., $I_{Ag} \propto I^0_{Ag} - \text{const} \times I_{oxy}$ with slopes of 8.8, 9.3, and 10.5, respectively. Hence it follows unambiguously that the O_γ species are located within the topmost layer, shielding the underlying Ag atoms from the He^+ ion beam.

D. Scanning tunneling microscopy

Using the STM technique and electrolytic silver particles as substrate, it was recently possible to obtain atomically resolved images of O_γ.[23] Figure 10 summarizes the results. On the (111) faces a hexagonal atomic arrangement was resolved, exhibiting deep holes in the center of each hexagon. The average interatomic distance between silver atoms is not markedly different from 2.85 Å, i.e., the structure is still a close-packed arrangement. If the holes are associated with oxygen atoms which cause the contrast by the steep variation in local work function (see Sec. III B) between the metallic surface and the isolated atoms, we can assign a ''bilayer'' structure to this species. Two hexagonal primitive lattices of silver and oxygen interpenetrate and sit upon a layer of close-packed silver atoms terminating the bulk. No information about the third dimension, i.e., the thickness of this bilayer, can be obtained from the STM information. Any degree of incomplete interpenetration is possible in principle.

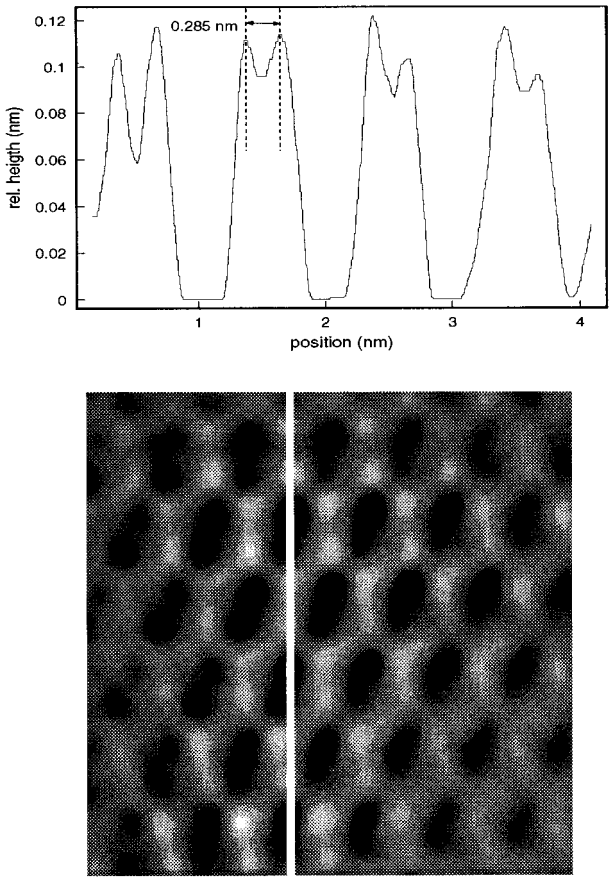

FIG. 10. Atomic-resolution STM image of the (111) side of a facet of an electrolytic silver particle after loading with oxygen. The interatomic distance of the silver atoms (light maxima) measured along the line indicated is 2.85 Å. The very large corrugation height through the hexagon of 1.0 Å is a clear indication of the influence of local electronic effects, and is no topographic property of the surface. For the same reason, the silver atoms appear to be much too small relative to the central atom. The asymmetry of the ''oxygen'' hole could be an indication for an off-center position caused by a noncoplanar arrangement of silver and oxygen in the top layer.

E. Reference oxide

In order to compare the spectral properties of the surface oxides with known bulk structures, we studied the photoemission from a sample of $Ag_7O_8NO_3$. This clathrate compound was chosen for its stability against contamination with carbon compounds and for its known decomposition behavior, allowing one to generate a clean variety of Ag_2O.[26,27] The material was synthesized by electrocrystallization of an acidic solution of $AgNO_3$ at a current density of 4 mA/cm^2 with a glassy carbon anode and a platinum cathode. The electrochemical reactions followed the scheme reported in the literature.[28]

The single-crystalline needles were used for an x-ray structure redetermination. *In situ* powder diffraction analysis of the decomposition reaction was performed with material crushed under Ar. The results can be summarized as follows. The phase-pure starting material (JCPDS no. 60437) decom-

posed at room temperature within 6 months and at 360 K within 2 h into AgO (JCPDS no. 220472) and at 410 K into Ag_2O (JCPDS no. 120793). The formation of crystalline phases of silver nitrate, silver carbonate, and other binary silver oxides could be ruled out. In the two-phase region of the thermogram in the literature[27] we detected reflections of elemental silver which grew in intensity and became single phase at 710 K. This picture of a silver excess in thermally degrading silver oxide is in agreement with a gas-solid reaction in which the silver migrates to metal nuclei and the oxygen desorbs from the surface. The growth of silver nuclei was also detected from a change in line profile of the silver reflections, which became narrower proportionally to the reaction progress.

The photoemission data were obtained from a sample of single crystals crushed in UHV at 300 K in a gold mortar. This preparation ensured a maximum of sample integrity. Controlling the composition of the atmosphere with a quadrupole mass spectrometer during crushing and subsequent x-ray illumination allowed us to ensure that no significant loss of volatiles (incorporated water, molecular oxygen) changed the surface constitution prior to controlled heating, which was done at a rate of 4 K/min. The measurement temperatures were chosen according to the x-ray investigation and the published Raman spectra[26] of the decomposition products. The spectra in Figs. 11, 12, and 13 in the state *A* were taken at 300 K and represent the starting oxide, the spectra in the state *B* were measured at 473 K after heating to 553 K and should represent Ag_2O, and the spectra in the state *C* were measured at 300 K after heating to 773 K and should represent metallic silver with dissolved/adsorbed residual oxygen according to the Raman data. The nitrate core level at 405.7 eV and the Raman band at 1040 cm^{-1} (not shown) indicate that the first decomposition step leads to the formation of x-ray-amorphous silver nitrate in addition to the binary oxide. For this reason, the spectra of measurement *B* will not be considered as reference here.

The surface composition in atomic percent agreed well for the starting compound with theoretical values (e.g., Ag: 37.9% found, 36% theory; N: 5.4% found, 5.2% theory). After decomposition to the metallic state the surface contained only 72.6 at. % silver, 0.0 at. % nitrogen, and 21.3 at. % oxygen, leading to a formal composition of $Ag_{3,4}O$. The accuracy of these data is, however, limited, as different data sets for the atomic cross sections exist which disagree in their results, mainly on the value for oxygen.

As $Ag_7O_8NO_3$ is a metallic material, the binding-energy data can be directly compared to the values for silver and the adsorbates without having to account for charging problems. The data in Table I agree well with the values for the binary oxide from Ref. 7 and also with the data for the O_γ phase. A more detailed comparison for the oxygen 1*s* region is presented in Fig. 11. The parent oxide spectrum of curve *a* of Fig. 11 (state *A*) exhibits two lines, the lower of which is unambiguously due to one oxide species in the compound. The main feature is a composite line with a significant contribution of OH species incorporated during synthesis of the compound. This was substantiated by the mass-spectral observation of water during heating the sample. The residual oxygen in the silver powder which gives rise to characteristic Raman bands occurs at 530.6 eV (Fig. 11, curve *b*), significantly lower than the main line of the as-prepared oxide. The asymmetry to lower binding energy indicates the presence of some strongly bound surface oxygen, as seen also in the Raman data. The spectra of the dissolved species and the initial oxide form are constituents of the complex spectra from the Ag(111) single crystal as exemplified by one spectrum from the sequence of Fig. 1 (see curve *c* of Fig. 11).

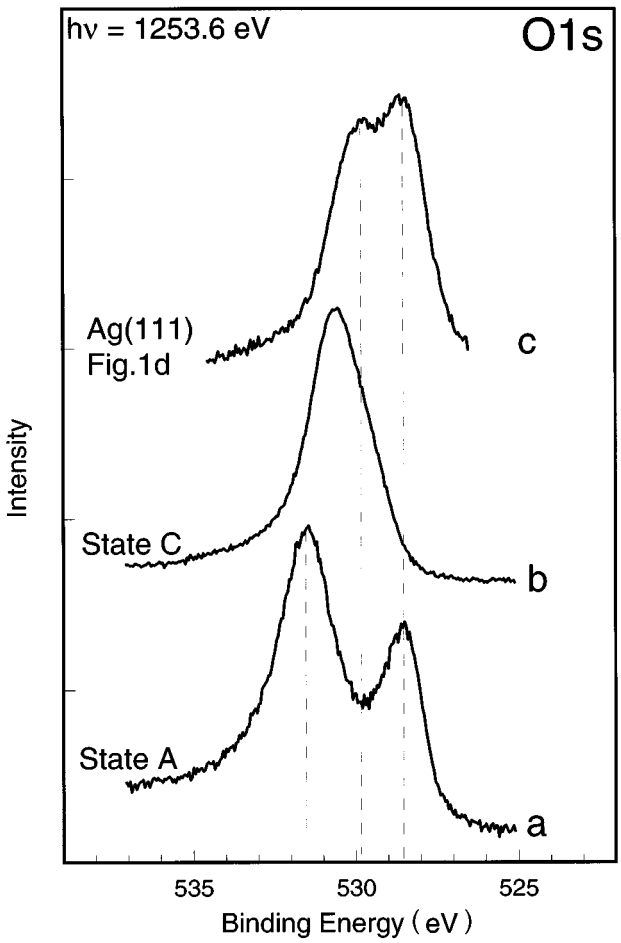

FIG. 11. O 1*s* core-level data from the reference oxide $Ag_7O_8NO_3$, (curve *a*) in the state *A* (bottom spectrum) of the starting oxide and (curve *b*) in the state *C* (middle spectrum) after heating to 770 K, representing the metallic silver with dissolved/adsorbed residual oxygen according to the Raman data (Ref. 26). The top spectrum *c* is taken from curve *d* of Fig. 1 and shows the O 1*s* core-level spectrum from a Ag(111) surface after exposure to 1 bar O_2 for 3 h at 780 K.

The Ag 3*d* spectra in Fig. 12 illustrate the negative binding-energy shift characteristic for silver oxides. The main line in state *A* is situated at the position of the difference peak in Fig. 4 at 367.3 eV binding energy, illustrating the validity of this data treatment. The broad line as well as the satellites (arrows) indicate the operation of final-state effects in the compound $Ag_7O_8NO_3$ and are not signs of a metallic silver surface contamination (remember the correct Ag:N ratio from the quantification). After transformation into the metal, the Ag 3*d* lines show the same narrow line profile as observed with the single crystal. The characteristic loss structures indicate the presence of a well-developed metallic electron system with no perturbation by the dissolved oxygen species. This can be taken as an indication that the

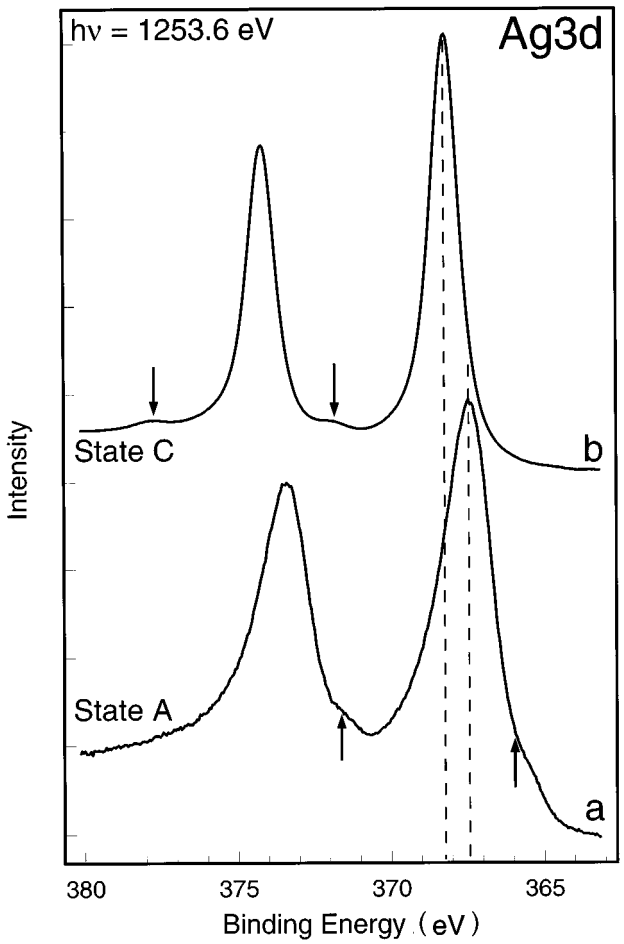

FIG. 12. Ag 3*d* core-level data from the reference oxide $Ag_7O_8NO_3$, (curve *a*) in the state *A* (bottom spectrum) of the starting oxide and (curve *b*) in the state *C* (top spectrum) after heating to 770 K, representing the metallic silver with dissolved/adsorbed residual oxygen according to the Raman data (Ref. 26).

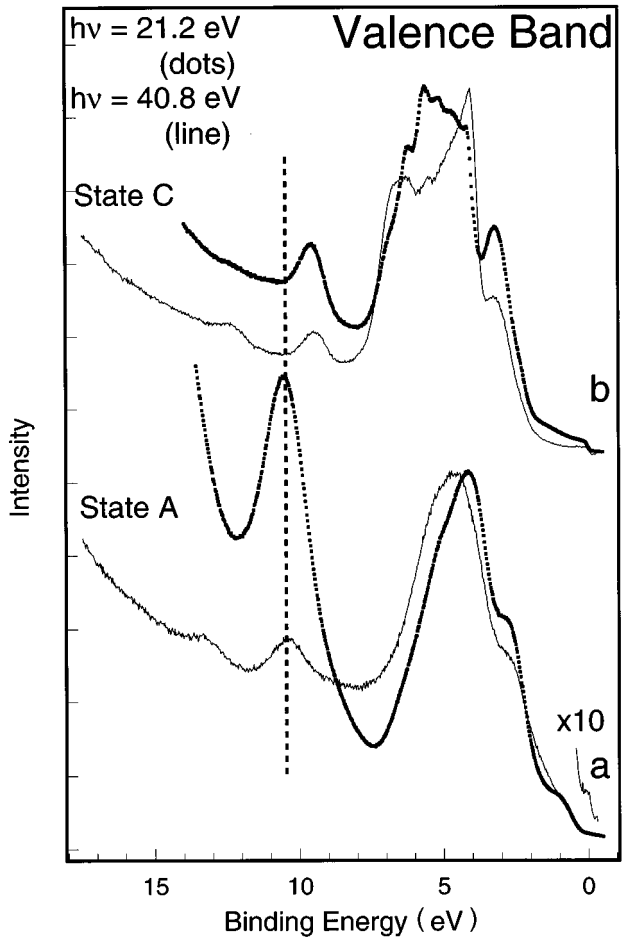

FIG. 13. Valence-band data excited with (curve *a*) He I ($h\nu$ =21.2 eV) (dotted spectra) and (curve *b*) He II ($h\nu$=40.8 eV) (line spectra) radiation from the reference oxide $Ag_7O_8NO_3$ in the state *A* (bottom spectra) of the starting oxide and in the state *C* (top spectra) after heating to 770 K, representing the metallic silver with dissolved/adsorbed residual oxygen according to the Raman data (Ref. 26).

type of chemical bonding interaction is not strongly interfering with the metal electronic structure.

The profoundly different electronic bonding interaction in the oxidic and oxygen-dissolved states is even more clearly seen in the valence-band photoemission data excited with He I (dotted spectra) and He II (line spectra) radiation displayed in Fig. 13. In the oxidic state the sample is metallic as can be seen from the small Fermi edge. The main features are, however, completely dissimilar from the metallic silver spectrum, as can be seen from comparison of states *A* and *C* in the figure and from inspection of Figs. 5 and 6. The intensity up to 7 eV below the Fermi edge is ascribed to predominantly silver 4*d*–derived hybrid states, as seen from the comparison of the relative cross-section variation between the excitations with He I and He II radiation. It is pointed out that the influence of hybridization between silver and oxygen states is drastic and removes any similarity of these spectra with the features of elemental silver. The doublet structure at 10.3 and 13.4 eV is associated with OH in the structure as seen already with the O 1*s* core-level spectrum, and as discussed with the spectra in Figs. 5 and 6. The intensity variation with excitation energy is exaggerated due to the drastic change in the background function which was not removed here. In the oxygen-dissolved state *C*, the OH groups remain at a different binding energy, indicating a different bonding interaction with the now metallic silver. This follows also from a reduced cross-section variation of the 9.6 eV feature. The silver *d*-band structures are more clearly resolved but still remain distorted by some underlying oxygen 2*p* features, as can be deduced again from the cross-section variation. The strong peak at 3.1 eV is reminiscent of the structure in Figs. 5 and 6 and illustrates that the double features at low binding energies in the single-crystal spectra are indicative of several species and do not represent a split state of a single oxygen species. As in chemisorption systems, the features at low binding energy in the spectrum from the oxygen-dissolved state *C* are of considerable *d*-state character and point qualitatively to the same type of chemical bonding interaction, which is in full agreement with the Raman observations.

In summary, the spectra of the reference oxide are similar to the chemisorption system and indicate the following point. Although there are several crystallographically different oxygen environments, the spectra do not contain unambiguous evidence for these oxygen species. Secondly, the spectra contain strong hints toward a nonionic chemical bonding

TABLE I. The binding and kinetic energies of the core levels, Ag $3d_{5/2}$ and O $1s$, the valence-band features in addition to the Ag $4d$ band, and the Auger electron lines Ag MNN and O KLL. The peak positions are measured from the spectra shown in Figs. 1–6 and 11–13 and from Ref. 7.

Surface	Ag $3d_{5/2}$ (eV)	O $1s$ (eV)	Ag MNN (eV)	O KLL (eV)	UPS[a] (eV)
Ag(111)	368.0		351.8		
Ag foil[b]	368.0		352.5		
Ag_2O[b]	367.6	528.9	351.9	515.9	2.8, 1.8
$Ag_7O_8NO_3$	367.4	528.6	352.4		2.9, 1.5,
		531.6			15.4, 10.5
Ag originate from $Ag_7O_8NO_3$	368.2	530.6	351.8		3.3, 1.3
					12.4, 9.6
Ag-O_γ	368.0	529.0		514.8	3.2, 2.5
	367.3				12.5, 9.8
Ag-O_β	368.0	530.3		511.3	3.2, 2.5
+Ag-O_α		530.4			

[a]Features in addition to the Ag $4d$ band.
[b]Reference 7.

with strong hybridization between silver $4d$ states and oxygen $2p$ states. The unusual low-binding-energy shift for the Ag $3d$ core level is confirmed with a bulk sample and agrees well with the data from a binary oxide film. Finally, it is noted that the sample contains substantial amounts of hydroxyl, which seems not to affect the existence of the clathrate compound. This would not be possible if the compound were purely ionic in its bonding interactions.

IV. DISCUSSION

A. Formation of the O_γ surface layer

The exposure of silver to oxygen leads at room temperature to the chemisorption of atomic oxygen on the surface, O_α, and to the slow incorporation of oxygen into the bulk, O_β. The dissolved oxygen atoms occupy interstitial octahedral sites of the silver lattice and leave the structural and electronic properties of metallic silver essentially unchanged. The chemisorbed oxygen atoms, however, capture electrons from the underlying silver atoms, which is reflected by the increase of the work function. The observed maximum value of the work function change is about 0.6 eV, which corresponds to a saturation coverage ($\Theta=0.5$) of the O_α species.[2]

When the exposure temperature is raised to a critical value, the oxygen atoms may undergo place exchange with metal atoms at the surface, increasing the work function by about 1 eV compared to clean silver. This process is accompanied by a 3% expansion of the lattice, which has been identified by RHEED, REM, and STM.[8] Such a surface oxidation process with mass transport of Ag atoms may occur significantly below the melting point if the cohesion energy of the exposed surface is low and the oxygen-metal bond is strong. During the growth of the oxidelike surface layer an intermediate situation exists, with all three types of atomic oxygen present. O_γ is associated with restructured islands detected[9] by REM coexisting with O_α on nonrestructured parts of the silver surface. Both O_α and O_γ can exchange with O_β depending on the temperature, leading to complex results when carrying out TDS experiments.[29]

As revealed by XPS and ISS, the rebuilding of the oxidelike layer after removal by sputtering can be achieved by the segregation of O_β oxygen transforming into O_γ. Such a transformation was found to occur at lower temperatures, for instance, at 500 K, although the exposure of an O_β-free Ag(111) surface to 1 bar oxygen at these temperatures would hardly create any O_γ oxygen. Hence the prehistory of the Ag sample is of crucial importance for the outcome of an oxygen-exposure experiment at high pressure and high temperature. It seems likely that the ''strongly bound oxygen'' associated with a $c(2\times2)$ LEED pattern observed in Ref. 24 on Ag(110) after 30 min oxygen exposure at 470 K is identical to O_γ in this study, as evidenced by the UPS, peak at 3.1 eV and the work function change of 1.2 eV.

B. Electronic and structural properties of the O_γ surface layer

The nature of the chemical bonding of the surface layer obtained on Ag(111) after prolonged oxygen exposure at 780 K and at atmospheric pressure is illustrated in Table I, comparing the results obtained in this study with the thick Ag_2O layer on Ag(111) produced by a free-radical oxygen source.[7] The similarity between the electron spectroscopic properties of the surface layer with incorporated O_γ and bulk Ag_2O suggests that at 780 K a surface layer which has oxidelike properties coexists with oxygen dissolved in the bulk, although the decomposition temperature of bulk Ag_2O has been exceeded by 160 K. Both the O $1s$ binding energy and the work function increase of about 1 eV indicate that O_γ is a negatively charged species.

From a chemical point of view such a Lewis-basic oxygen species embedded in the topmost layer should have a high reactivity toward adsorption of polar molecules and dehydrogenation reactions of Lewis-acidic substrates. Indeed, the UPS and XPS results reveal the presence of OH groups after high-pressure dosing. It has been shown recently by *in situ* Raman spectroscopy that the presence of water actually favors the formation of the O_γ species.[26] *In situ* Raman measurements also revealed that O_γ is present under typical methanol dehydrogenation conditions, reacting readily with

methanol. By exposing polycrystalline silver grains to a methane- and oxygen-containing feed at about 1000 K, it was possible to couple methane to C_2 hydrocarbons.[30] These catalytic observations support the suggested Lewis-basic properties of the oxidelike surface layer, rendering silver an efficient oxidation-dehydrogenation catalyst.

Using the analogy to copper, the O_γ-containing surface layer might actually be identified structurally as an epitactic thin $Ag_2O(111)$ overlayer. This was suggested as early as 1974 by Rovida *et al.*[31] and in more detail by Campbell.[5] Campbell discusses the possibility that one ''trilayer'' consisting of a hexagonal Ag layer surrounded by two hexagonal oxygen layers with a thickness of about 2.7 Å may be present on top of Ag(111) after dosing with several mbar of oxygen at 490 K. This ''trilayer'' model is in fair agreement with the estimated monolayer thickness of the oxidelike layer and the location of O_γ in the topmost layer shielding the underlying silver layers as shown by ISS. The present model is a ''bilayer'' structure, with silver and oxygen coexisting within one layer but with unknown corrugation.

The low stability of the hexagonal polymorph of Ag_2O (see below) allows us to exclude the possibility that the oxygen and silver atoms are just simply stacked upon each other. The suggested interpenetration model is consistent with the XPS and ISS observations. Its formation is possible as the atomic radius of silver and the van der Waals radius of an oxygen atom are almost identical and allow substitution without large lattice deformations. The small lattice expansion of ca. 3% leading to the moiré pattern in REM which is also seen in the STM images indicates the good match of the two atomic species. It is interesting to note that the van der Waals radius of oxygen and the ionic radius for an oxide anion are at 1.38 and 1.40 Å almost identical to the atomic radius of silver at 1.44 Å, whereas a silver cation Ag^+ fills only a sphere with 1.13 Å radius.

These data set limits on the degree of charge transfer between oxygen and silver, which is better described by a hybridization of Ag $4d/5s$ states with the valence band of silver than by an oxidic bonding between ions of Ag^+ and O^{2-}. Such a hybridization is well in line with the structure of the valence bands seen in Figs. 5 and 6, where most of the oxygen-band intensity is located overlapping with the silver d-band feature. Also the fact that the core-level shift for the silver atoms directly surrounding the oxygen atoms is shifted to low binding energies and not to higher binding energies is not in contrast with the conjecture that the ionic contributions to the chemical bonding are limited. In addition, if the oxygen-surrounding silver atoms carried a significant positive charge, we should expect a non-close-packing of species with the same sign of electrostatic charge. The importance of covalent bonding with a strong mixing of metal d states and oxygen s/p states was also found from systematic[32] and silver-specific[33] x-ray absorption studies. In the latter study a white line was found in the Ag L, edge spectra of oxidic compounds, the existence of which excludes the closed-shell structure of the Ag $4d^{10}$ band. The interpretation given in this paper[33] that the intensity of the white line should be proportional to the oxidation state of the silver can be reanalyzed in terms of a changing hybridization of the Ag $4d$ states with the different ligand systems. In the silver-oxygen chemisorption system the type of chemical bonding seems to be different for the three oxygen species. This variation in interaction between the formally similar silver-oxygen atom groups finds its parallel in three-dimensional bulk oxides. The reference compound $Ag_7O_8NO_3$ was chosen as it contains two different oxidation states (Ag^+ and Ag^{3+}) of silver within each unit cell. It is a silver-rich oxide of the clathrate type with a three-dimensional Ag-O polyhedral network (a cuboctahedron).[34] This formal bonding concept (comprising Ag^{3+} and O^{2-} ions in a square planar coordination) is based upon the assumption that oxygen is always present as the oxoanion O^{2-} and that different structural environments are caused by different ionic charges of the constituents.[35] The different structural environments lead to different Ag-O distances of 2.52 and 2.05 Å, leading to ionic radii of 1.26 Å for Ag^+ and of 0.76 Å for Ag^{3+}. The difference in interatomic distances is large enough within this homogeneous bulk compound to call for significantly modified electronic interactions within each unit cell. It is, however, not necessary to invoke large variations in the localized charge distributions between silver and oxygen as is done in the ionic concept of bonding, leading to the necessity of postulating a special cation-cation bonding force[36] in order to account for the close packing of the silver ''cations'' in such compounds. Alternatively, the concept of covalent interaction involving either only Ag $5s$ states or Ag $4d/5s$ states may equally account for different bonding geometries and bonding distances, without having to separate different numbers of electronic charges between neighboring atoms. In order to avoid the idea of ionic bonding with large charge transfers, we hesitate to use the term ''oxidelike'' bonding state for the $Ag\text{-}O_\gamma$.

In a recent proposal of Ag_2O being an important surface structure for the ethylene epoxidation silver catalyst[37] a fully ionic bonding structure was assumed. This was required for the analysis of the solid state electrochemistry, proving the availability of oxide anions at the surface of this oxide at 440 K and 75 bar hydrostatic pressure. As pointed out in this paper, the oxide structure cannot be responsible for the catalytic action in the methanol conversion reaction as the dissociation pressure at 900 K under thermodynamic equilibrium would be above 1000 bar.[38] In this context it is pointed out that in a recent study[7] of the nature of the bonding in Ag_2O a significant covalent interaction was stated, but an essentially closed shell for the Ag $4d$ states was also concluded from spectroscopic arguments. The detection of a white line in the Ag L_3 edge spectra can thus only be seen as strong support for the present conjecture of an important covalent interaction in silver oxides. The comparison of valence-band photoemission with x-ray absorption spectroscopy in combination with suitable calculations on the structure of $Ag(111)\text{-}O_\gamma$ will be reported elsewhere and is in full agreement with the presented ideas.

Returning to the structural properties of $Ag(111)\text{-}O_\gamma$, we state that the interpenetration model is a unique surface structure and can exist only as a two-dimensional entity. The structural motif of a silver-oxygen bilayer occurs as a three-dimensional structure in the hexagonal polymorph of Ag_2O, a structural model of which is shown in Fig. 14.[39] The bonding distances of Ag-Ag and Ag-O are at 3.07 and with 2.16 Å quite different from each other, and indicate significant charge transfer with a non-close-packing of the partly ionic

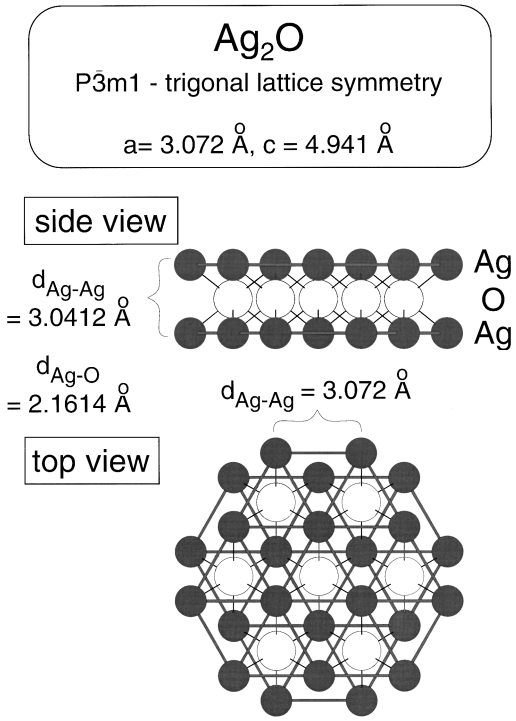

FIG. 14. A hexagonal structural model of Ag_2O is shown (Ref. 39). The bonding distances of Ag-Ag and Ag-O are, at 3.07 and 2.16 Å, quite different from each other, and indicate significant charge transfer with a non-close-packing of the partly ionic silver atoms.

silver atoms. The Ag-O distance is, however, significantly shorter than the sum of the hard-sphere ionic radii at 2.51 Å. This indicates that the structure is not fully ionic, but contains significant hybridization interactions, leading to smaller oxygen radii and less positive repulsion between the silver atoms. The oxygen atoms are situated deep within the threefold hollow site of the silver networks, as follows from the interlayer silver-silver distance of 3.04 Å, which is only 0.20 Å larger than the sum of the atomic radii. The bonding distances in the Ag(111)-O_γ structure are ideally at 2.85 Å for both interactions of the same length and indicate a chemical bonding interaction with less charge transfer than in Ag_2O (with a significant error margin of the STM method). These structural data can be compared to the experimentally determined surface structure of silver-oxygen on the (110) face, which is shown in Fig. 15.[40] The Ag-Ag distance is at 2.89 Å similar to that in the other structures. It indicates a close packing of the metal atoms and remains essentially unchanged by the nature and abundance of the nonmetal atoms. The Ag-O distances are, at 2.05 Å to the in-plane neighbors and 2.12 Å to the underlying silver atoms, significantly shorter than in the oxide structures. Their values indicate a significant charge transfer with a considerable ionic character of the atoms. In this surface structure the silver seems to behave like an alkali-metal ion. The bonding situation may be caused by the incorrect geometric arrangement for an efficient orbital overlap of the Ag $4d$ states with the oxygen p states on the (110) surface.

A covalent interaction seems to be more favored on the (111) face, as may be deduced by the observation that every silver surface restructures into (111) provided that the oxy-

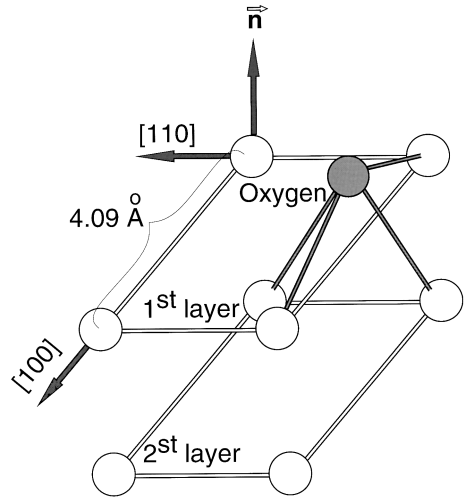

FIG. 15. Schematic adlayer structure of Ag(110)-O(2×1) showing the oxygen atoms on bridge sites in the [100] direction above the surface Ag atoms (after Ref. 40). The Ag-Ag distance is at 2.89 Å similar to that in the hexagonal structural model of Ag_2O.

gen partial pressure is sufficiently high. The questions arise as to why this silver-oxygen interaction is more stable than any three-dimensional oxide structure, and why the hexagonal Ag_2O structure does not contain the same chemical interaction as the surface oxygen phase. The second question may be answered by considering the conditions of the formation of the O_γ phase, which requires temperatures of about 500 K, above the stability limits for all known binary oxides at ambient pressure of oxygen. Increasing the oxygen partial pressure with elemental silver may not be sufficient to create the desired oxide phases, as an efficient competition exists between oxidation and diffusion of neutral oxygen atoms through the silver lattice. The same oxygen mobility was also recently observed by solid state electrochemistry at elevated temperatures and pressures, which were, however, not high enough to overcome the threshold for O_γ formation.[34] Furthermore, an *in situ* UPS and XPS study of evaporated silver films as an oxygen electrode material[41] performed at temperatures between 720 and 1100 K revealed oxygen species at the surface and at the sub-surface sites under anodic polarization with steady-state oxygen evolution. The latter oxygen species was attributed to oxygen atoms dissolved in the bulk, and the further oxygen species at low binding energy was assigned to strongly adsorbed oxygen atoms. This means that the observed surface-oxygen structure may have a bulk analogue—an as yet unknown high-pressure phase of Ag_2O. The underlying reason would be that the activation energy to change the electronic configuration of the closed silver $4d^{10}$ shell into a metal-ligand hybrid state is too large with respect to bulk phase segregation into the elements silver and oxygen.

On the Ag(111) surface this may be different for two reasons. First, the activation energy for the electronic modification of the surface silver atoms will be different from the bulk value due to the coordinative undersaturation. Second, the surface electrostatic field will stabilize its origin, i.e., will form a barrier for the back-diffusion of the silver into the bulk, a process which is required for the decomposition of an oxide. The drastic change in work function associated with

the formation of the Ag(111)-O_γ phase (see Sec. III B) is an indication of the strength of this surface field. The effect of the surface electrostatic field on the mobility of ions may be estimated quantitatively from the theory of Cabrera and Mott,[42] which was, however, not developed for the high-temperature condition applying here. Using the work function change of 1.0 eV as estimate of the field and assuming a 5.0 Å thick ''oxide'' layer and a jump distance of a silver ion of the same length, an increase of 60 kJ/mol in activation energy for the jump motion of silver ions would result.

The magnitude of these electrostatic effects and the spectral parameters of the O_γ species raise a question about the nature of the electronic interaction from a different point of view than discussed above. Intuitively, one would take the work function change, the STM contrast, and the very low binding energies in the O 1*s* core level and in the valence band as indications for a strongly negative local charge on the oxygen ions. The similarity of the spectral parameters between the surface compound and the bulk reference oxide further supports this conjecture. Indicators for a more subtle type of chemical interaction are, however, the structural details, deviating significantly from an ionic close packing as outlined above. These data render the interpretation of the Ag L_3 x-ray absorption data in terms of ionic open *d*-shell structures unlikely. Also, the valence-band UPS data shown in this work are incompatible with an ionic rigid-band behavior of all species of the surface-bound oxygen.

We arrive at the following concluding description of the system. First, we note that the silver-oxygen system can form chemical interactions of significantly different nature as bulk compounds and as surface species. In classical solid state chemistry, this ambivalence finds its parallel in silver compounds where silver behaves like an alkali-metal ion and other silver compounds, in which unusual d^{10}-d^{10} bonding forces have to be invoked to explain the observed crystal structures.[35,36] In the present surface chemical system, the O_α species represents the ionic extreme. Here the interaction is mainly limited to Ag $5sp$/O $2p$ overlaps, with a significant charge transfer to the oxygen leading to the observed work function change, the O $2p$ signature in the valence band as a peak below the Ag $4d$ band, and an O 1*s* core-level binding energy of about 530.5 eV, which is fully compatible with most other transition-metal oxide data.[20] Increasing temperatures and oxygen partial pressures open two reaction channels for the adsorbate in addition to recombination and desorption. In silver, it is energetically relatively cheap for oxygen to become dissolved in the bulk of the substrate as O_β. This is indicated by the significant oxygen mobility through silver foils[43] and is also not unusual with noble-metal systems, as the example of the Pd-O system shows.[44] This example illustrates that the system reacts upon further increase of the chemical potential of oxygen by formation of binary oxides with bulk structures. The thresholds for oxidation are governed by the steps required to intensify the orbital interaction from a metal s/p–oxygen p interaction to a metal $s/p/d$–oxygen p interaction. This process is easier for open *d*-shell metals than for closed *d*-shell metals like silver. The transition into a covalent oxide occurs for this element only as a one-monolayer structure identified as O_γ. The bulk oxides such as Ag_2O represent the more ionic interaction with oxygen, whereas in the reference oxide $Ag_7O_8NO_3$ both types of bonding coexist. The higher-coordinated cubic silver sites represent the covalent bonding situation and the lower-coordinated square planar environment occurs from the ionic situation.

The spectroscopic properties of O_γ such as the significant additional increase in work function, the complex valence-band pattern with pronounced convolutions of the silver *d*-band features with the oxygen *p*-band states, the unusual silver $3d$ shift, and the very low oxygen $2p$ binding energy do not indicate an isolated O^{2-} species, but are consistent with a layer of Ag-O interactions, which may be symbolized chemically by a Ag═O double bond. The formation of this covalent hybrid interaction requires spatial registry between oxygen and silver states and is thus structure sensitive. Theoretical work presented in a forthcoming publication will illustrate this spatial requirement and the energetic consequences of its fulfillment.[45] It is noted that the discrimination of the chemical interaction into ''ionic'' and ''covalent'' is crude, and reference is given to a discussion of the substantial degree of covalent interaction in binary transition-metal oxides.[32]

ACKNOWLEDGMENTS

We are indebted to the group of Professor E. W. Grabner, University of Frankfurt, for the help with the preparation of the reference oxide. This work was financially supported by the BASF AG Ludwigshafen.

*Author to whom correspondence should be addressed. FAX: ++49-30-8413-4401. Electronic address: thomas@carbon.rz-berlin.mpg.de

[1] R. A. van Santen and H. P. C. E. Kuipers, Adv. Catal. **35**, 265 (1987).

[2] M. A. Barteau and R. J. Madix, in *The Chemical Physics of Solid Surfaces and Heterogeneous Catalysis*, edited by D. A. King and B. P. Woodruff (Elsevier, Amsterdam, 1982), Vol. 4, Chap. 4.

[3] K. C. Prince, G. Paolucci, and A. M. Bradshaw, Surf. Sci. **175**, 101 (1986).

[4] H. Schubert, U. Tegtmeyer, and R. Schlögl, Catal. Lett. **28**, 383 (1994).

[5] C. T. Campbell, Surf. Sci. **157**, 43 (1985).

[6] M. Bowker, Surf. Sci. **155**, L276 (1985).

[7] L. H. Tjeng, M. B. Meinders, J. van Elp, J. Ghijsen, G. A. Sawatzky, and R. L. Johnson, Phys. Rev. B **41**, 3190 (1990).

[8] X. Bao, J. V. Barth, G. Lehmpfuhl, R. Schuster, Y. Uchida, R. Schlögl, and G. Ertl, Surf. Sci. **284**, 14 (1993).

[9] X. Bao, M. Muhler, B. Pettinger, R. Schlögl, and G. Ertl, Catal. Lett. **22**, 215 (1993).

[10] X. Bao, B. Pettinger, G. Ertl, and R. Schlögl, Ber. Bunsenges. Phys. Chem. **97**, 322 (1993).

[11] C. Rehren, M. Muhler, X. Bao, R. Schlögl, and G. Ertl, Z. Phys. Chem. **174**, 11 (1991).

[12] J. J. Yeh and I. Lindau, At. Data Nucl. Data Tables **32**, 1 (1985).

[13] G. Ertl and J. Küppers, *Low Energy Electrons and Surface Chemistry* (Verlag Chemie, Weinheim, 1985).

[14] C. T. Campbell and M. T. Paffett, Surf. Sci. **143**, 517 (1984).
[15] M. A. Barteau and R. J. Madix, J. Electron Spectrosc. Relat. Phenom. **31**, 101 (1983).
[16] R. W. Joyner and M. W. Roberts, Chem. Phys. Lett. **60**, 459 (1979).
[17] R. B. Grant and R. M. Lambert, Surf. Sci. **146**, 256 (1984).
[18] K. Siegbahn, C. Nording, G. Johansson, J. Hedman, P. F. Heden, K. Hamrin, U. Gelius, T. Bergmark, L. O. Werme, R. Manne, and Y. Baer, *ESCA Applied to Free Molecules* (North-Holland, Amsterdam, 1969).
[19] X. Bao, G. Lehmpfuhl, G. Weinberg, R. Schlögl, and G. Ertl, J. Chem. Soc. Faraday Trans. **88**, 865 (1992).
[20] K. Wandelt, Surf. Sci. Rep. **2**, 1 (1982).
[21] D. Briggs and M. P. Seah, Pract. Surf. Anal. **1**, 209 (1990).
[22] L. H. Tjeng, M. B. Meinders, and G. A. Sawatzky, Surf. Sci. **236**, 341 (1990).
[23] H. Schubert, U. Tegtmeyer, D. Herein, X. Bao, M. Muhler, and R. Schlögl, Catal. Lett. **33**, 305 (1995).
[24] W. Segeth, J. H. Wijngaard, and G. A. Sawatzky, Surf. Sci. **194**, 615 (1988).
[25] H. Niehus, W. Heiland, and E. Taglauer, Surf. Sci. Rep. **17**, 213 (1993).
[26] B. Pettinger, X. Bao, I. Wilcock, M. Muhler, R. Schlögl, and G. Ertl, Angew. Chem. Int. Ed. Engl. **33**, 85 (1994).
[27] I. Naray-Szabo and K. Popp, Z. Anorg. Allg. Chem. **322**, 286 (1963).
[28] J. A. McMillan, Chem. Rev. **62**, 65 (1962).
[29] C. Rehren, G. Isaac, R. Schlögl, and G. Ertl, Catal. Lett. **11**, 253 (1991).
[30] X. Bao, M. Muhler, R. Schlögl, and G. Ertl (unpublished).
[31] G. Rovida, F. Praseti, M. Maglietta, and E. Ferroni, Surf. Sci. **43**, 230 (1974).
[32] F. M. F. de Groot, M. Grioni, J. C. Fuggle, J. Ghijsen, G. A. Sawatzky, and H. Petersen, Phys. Rev. B **40**, 5715 (1989).
[33] P. Behrens, Solid State Commun. **81**, 235 (1992).
[34] I. Naray-Szabo, G. Argay, and P. Szabo, Acta Crystallogr. **19**, 180 (1965).
[35] M. Jansen, J. Less Common Met. **76**, 285 (1980).
[36] M. Jansen and K. Heidebrecht, in *Unkonventionelle Wechselwirkungen in der Chemie metallischer Elemente*, edited by B. Krebs (VCH Verlag, Weinheim, 1992), p. 428.
[37] A. Wöhnke, R. Haul, and K. Schmalzried, Z. Phys. Chem. **186**, 215 (1994).
[38] Y. I. Gersasimov, Thermodyn. Nonferrous Met. **2**, 1 (1961).
[39] S. S. Kabalkina, S. V. Popova, R. N. Serebyanaya, and L. F. Verschchagin, Dokl. Akad. Nauk. SSSR **152**, 853 (1963).
[40] A. Puschmann and J. Haase, Surf. Sci. **144**, 559 (1984).
[41] W. Zipprich, H.-D. Wiemhöfer, U. Vohrer, and W. Göpel, Ber. Bunsenges. Phys. Chem. **99**, 1406 (1995).
[42] N. Cabrera and N. F. Mott, Rep. Prog. Phys. **12**, 163 (1948–1949).
[43] G. B. Hoflund, M. R. Davidson, and R. A. Outlaw, Surf. Interface Anal. **19**, 325 (1992).
[44] H. Conrad, G. Ertl, J. Küppers, and E. Latta, Surf. Sci. **65**, 245 (1977).
[45] Th. Schedel Niedrig, X. Bao, M. Muhler, and R. Schlögl (unpublished).